Atmos. Chem. Phys. Discuss., 15, 34205–34241, 2015
www.atmos-chem-phys-discuss.net/15/34205/2015/
doi:10.5194/acpd-15-34205-2015

Atmospheric Chemistry and Physics Discussions
Open Access
EGU

Influence of meteorology and interrelationship with greenhouse gases (CO_2 and CH_4) at a sub-urban site of India

G. Sreenivas, P. Mahesh, J. Subin, A. L. Kanchana, P. V. N. Rao, and V. K. Dadhwal

Atmospheric and Climate Sciences Group (ACSG), Earth and ClimateScience Area (ECSA), National Remote Sensing Center (NRSC), Indian Space Research Organization (ISRO), Hyderabad, 500037, India

Received: 28 October 2015 – Accepted: 21 November 2015 – Published: 4 December 2015

Correspondence to: P. Mahesh (mahi952@gmail.com)

Published by Copernicus Publications on behalf of the European Geosciences Union.

Abstract

Atmospheric greenhouse gases (GHGs) such as carbon dioxide (CO_2) and methane (CH_4) are important climate forcing agents due to their significant impact on the climate system. The present study brings out first continuous measurements of atmospheric GHG's using high precision Los Gatos Research's-greenhouse gas analyser (LGR-GGA) over Shadnagar, a suburban site of Central India during the period 2014. The annual mean of CO_2 and CH_4 over the study region is found to be 394 ± 2.92 and 1.92 ± 0.07 ppm (mean, $\mu \pm 1$ SD, σ) respectively. CO_2 and CH_4 showed a significant seasonal variation during the study period with maximum (minimum) CO_2 observed during Pre-monsoon (Monsoon), while CH_4 recorded maximum during post-monsoon and minimum in monsoon. A consistent diurnal mixing ratio of these gases is observed with high (low) during night (afternoon) hours throughout the study period. Influences of prevailing meteorology (air temperature, wind speed, wind direction and relative humidity) on GHG's have also been investigated. CO_2 and CH_4 showed a strong positive correlation during winter, pre-monsoon, monsoon and post-monsoon with R equal to 0.80, 0.80, 0.61 and 0.72 respectively. It implies the seasonal variations in source-sink mechanisms of CO_2 and CH_4. Present study also confirms implicitly the presence OH radicals as a major sink of CH_4 over the study region.

1 Introduction

The Intergovernmental Panel on Climate Change (IPCC, 2013) reported that humankind is causing globalwarming through the emission of greenhouse gases (GHG),particularly carbon dioxide (CO_2) and methane (CH_4). CO_2 and CH_4 concentrations have increased by 40 and 150 % respectively since pre-industrial times, mainly from fossil fuel emissionsand secondarily from net land use change emissions (IPCC, 2013). CO_2 measurements at Mauna Loa, Hawaii (Monastersky, 2013) have exceeded the 400 ppm mark several times in May 2013. CH_4 is also receiving increasing attention

ACPD
15, 34205–34241, 2015

due to high uncertainty in its sources and sinks (Keppler et al., 2006; Miller et al., 2007; Frankenberg et al., 2008). Kirschke et al. (2013) reported that in India, agriculture and waste constitutes the single largest regional source of CH_4. Although many sources and sinks have been identified for CH_4, their relative contribution to atmospheric CH_4 is still uncertain (Garg et al., 2001; Kirschke et al., 2013). In India, electric power generation that contributes to half of India's total CO_2 equivalent emissions (Garg et al., 2001).

Global climate change has serious impact on humans andecosystems. Due to this, many factors have been identified that may reflector cause variations in environmental change (Pielke et al., 2002). Out of these, the Normalized Difference Vegetation Index (NDVI) has become one of the most widely used indices to represent the biosphere influence on global change (Yang et al., 2011). The planetary boundary layer (PBL) is the part of the atmosphere closest to the Earth's surface where turbulent processes often dominatethe vertical redistribution of sensible heat, moisture, momentum, and aerosols/pollution (Ao et al., 2012).

Greenhouse and other trace gases have great importance in atmospheric chemistry and for radiation budget of the atmosphere–biosphere system (Crutzen et al., 1991). Hydroxyl radicals ($\dot{O}H$) are very reactive oxidizing agents, which are responsible for the oxidation of almost all gases that are emitted by natural and anthropogenic activities in the atmosphere. Atmospheric CO_2 measurements are very important for understanding the carbon cycle because CO_2 mixing ratios in the atmosphere are strongly affected by photosynthesis, respiration, oxidation of organic matter, biomass and fossil fuel burning, and air–sea exchange process (Machida et al., 2003).

The present study brings out first continuous measurements of atmospheric GHG's using high precision Los Gatos Research's-greenhouse gas analyser (LGR-GGA) over Shadnagar, a suburban site of Central India during the period 2014. In addition to GHG's observations, we have also made use of an automatic weather station (AWS) data along with model/satellite retrieved observation during the study period. Details about study area and data sets are described in the following sections.

ACPD
15, 34205–34241, 2015

2 Study area

Shadnagar is situated in Mahabubnagar district of newly formed Indian state of Telangana. It is a rural location situated ∼ 70 km away from urban site of Hyderabad (Northern side) with a population of ∼ 0.158 million (Patil et al., 2013). A schematic map of study area is shown in Fig. 1a. Major source of pollutants over Shadnagar can be from small and medium scale industries, biomass burning and bio-fuel aswell as from domestic cooking. In the present study sampling of GHG's and related meteorological parameters are carried out in the premises of National Remote Sensing Center (NRSC), Shadnagar Campus (17°02′ N, 78°11′ E). Sampling site is near to National highway 7 (NH7) and a railway track (non-electrified) is in the East (E) direction.

Mean monthly variations of temperature (°C) and RH (%) observed at Shadnagar during 2014 are shown in Fig. 1b and c respectively. The Indian Meteorological Department (IMD) defined monsoon as June–July–August–September (JJAS), post-monsoon (October–November–December – OND), winter (January–February – JF) and pre-monsoon (March–April–May – MAM) in India. Temperature over Shadnagar varies from ∼ 20 to ∼ 29°C. Relative humidity (RH) in Shadnagar reached a maximum of 82 % in monsoon from a minimum of 48 % recorded during pre-monsoon. Surface wind speed (Fig. 1d) varies between 1.3 to 1.6 $m\,s^{-1}$ with a maximum observed during monsoon and minimum in pre-monsoon. The air mass advecting (Fig. 1e) towards study site is either easterly or westerly. The easterly wind prevails during winter and gradually shifts to south-westerlies in pre-monsoon, and dominates during monsoon.

3 Data set and methodology

Details about the instrument and data utilized are discussed in this section. The availability and frequency of the observations all data used in present study are tabulated in Table 1.

ACPD
15, 34205–34241, 2015

3.1 In-situ observations

3.1.1 Greenhouse Gas Analyser (GGA)

The Greenhouse Gas Analyser (model: LGR-GGA-24EP) is an advanced instrument capable of simultaneous measurements of CO_2, CH_4 and H_2O. This instrument is well known for high precision and accuracy which are crucial towards understanding background concentrations of atmospheric GHGs, with specifications meeting WMO standards of measurement. It is based on enhanced Off-Axis Integrated Cavity Output Spectroscopy (OA-ICOS) technology (Paul et al., 2001; Baer et al., 2002), which utilizes true wavelength scanning to record fully resolved absorption line shapes. Considering the rural nature of the site, flow rateis fixed to be 7 liters per minute ($L\,m^{-1}$). Ambient air entering the GGA is analysed using two near infrared (NIR) distributed feedback tunable diode lasers (TDL), one for a CO_2 absorption line near 1.60 µm ($\nu_0 = 6250\,cm^{-1}$) and the other to probe CH_4 and H_2O absorption lines near 1.65 µm ($\nu_0 = 6060.60\,cm^{-1}$). The concentration of the gases is determined by the absorption of their respective characteristic absorption lines with a high sampling time of 1 s. A detailed explanation regarding the configuration, working and calibration procedure performed for GGA in NRSC can be found elsewhere in Mahesh et al. (2015). In the present study we used GGA retrieved CO_2 and CH_4 data. High resolution data are diurnally averaged and is used in further analysis. Due to failure of internal central processing unit (CPU) of the analyzer data is not recorded from pre-monsoon month of May to a few days in June during the study period.

3.1.2 O_3 and NO_x analyzer

Surface concentrations of O_3 and NO_x have been measured continuously using on-line analyzers Model No.s: 49i and 42i for O_3 and NO_x respectively, procured from Thermo Scientific, USA) since July 2014. The ozone analyzer is based on Beer–Lambert–Baugher law which relates absorption of light to the concentration of species as its

ACPD
15, 34205–34241, 2015

operating principle and has an in-built calibration unit for conducting periodical span and zero checks. The NO_x analyzer utilizes a molybdenumconverter to convert NO_2 into NO and estimates the NO_x concentration by the intensity of light emitted during the chemiluminescent reaction of NO with O_3 present in the ambient air. The analyzer is integrated with zero and span calibration which are performed twice monthly.

Simultaneous observations of meteorological parameters are obtained from an automatic weather stations (AWS) located in the same campus.

3.2 Satellite and model observations

3.2.1 MODIS

Moderate-resolution Imaging Spectrometer (MODIS) is launched in December 1999 on the polar-orbiting NASA-EOS Terra platform (Salomonson et al., 1989; King et al., 1992). It has 36 spectral channels and acquires data in 3 spatial resolutions of 250, 500 m, and 1 km (channels 8–36), covering the visible, near-infrared, short-wave infrared, and thermal-infrared bands. In the present study we used monthly Normalised Difference Vegetation Index (NDVI) data obtained from Terra/MODIS at 5 km spatial resolution. The NDVI value is defined as following ratio of albedos (α) at different wavelengths:

$$\mathrm{NDVI} = \frac{\alpha_{0.86\,\mu\mathrm{m}} + \alpha_{0.67\,\mu\mathrm{m}}}{\alpha_{0.86\,\mu\mathrm{m}} - \alpha_{0.67\,\mu\mathrm{m}}} \tag{1}$$

NDVI values can range from −1.0 to 1.0 but typical ranges are from 0.1 to 0.7, with higher values associated with greater density and greenness of plant canopies. More details of the processing methods used in generating the data set can be found in James and Kalluri (1994).

ACPD
15, 34205–34241, 2015

3.2.2 COSMIS-RO

COSMIC (Constellation Observation System for Meteorology, Ionosphere and Climate) is a GPS (Global Positioning System) radio occultation (RO) observation system (Wang et al., 2013). It consists of six identical microsatellites, and was launched successfully on 14 April 2006. GPS radio occultation observation has the advantage of near-global coverage, all-weather capability, high vertical resolution, high accuracy and self-calibration (Yunck et al., 2000). Geophysical parameters like temperature and humidity profiles have been simultaneously obtained from refractivity data using one-dimensional variational (1DVAR) analysis. Further COSMIC-RO profiles are used to estimate planetary boundary layer height (BLH). BLH is defined to be the height at which the vertical gradient of the refractivity or water vapor partial pressure is minimum (Ao et al., 2012), explained detail methodology for calculating the BLH from refractivity (N).

3.2.3 Hysplit model

The general air mass pathway reaching over Shadnagar is analysed using HYSPLIT model (Draxler and Rolph, 2003) (http://www.arl.noaa.gov/ready/hysplit4.html). We computed 5 day isentropic model backward air mass trajectory for all study days with each trajectory starting at 06:00 UTC and reaching study site, (Shadnagar) at different altitudes(1, 2, 3 and 4 km). Even though the trajectory analysis have inherent uncertainties (Stohl, 1998), they are quite useful in determining long range circulation.

4 Results and discussion

4.1 Seasonal variations of CO_2 and CH_4

Monthly variations of CO_2 and CH_4 during the study period are shown in Fig. 2a and b. Annual mean of CO_2 over study region is found to be 394 ± 2.92 ($\mu \pm 1\sigma$) ppm with an observed minimum in monsoon and maximum in pre-monsoon. Background (average) values of CO_2 observed during different seasons are 393 ± 5.60, 398 ± 7.60, and 392 ± 7.0 and 393 ± 7.0 ppm with respectively winter, pre-monsoon, monsoon and post-monsoon. Minimum CO_2 during winter (dry season) indicates the loss of carbon (Gilmanov et al., 2004) as decreased temperature and solar radiation during this period inhibit increases in local CO_2 assimilation (Thum et al., 2009). Enhancement in Pre-monsoon is due to higher temperature and solar radiation prevailing during these months which stimulate the assimilation of CO_2 in the daytime and respiration in the night (Fang et al., 2014). Surface CO_2 concentration recorded a minimum during monsoon months can be mainly because of enhanced photosynthesis processes with the availability of greater soil moisture (Patil et al., 2013). Further increase during post-monsoon CO_2 is associated with high ecosystem productivity (Sharma et al., 2014) also an enhancement in soil microbial activity (Kirschke et al., 2013).

CH_4 concentration in the troposphere is principally determined by a balance between surface emission and destruction by hydroxyl radicals ($\dot{OH}$). The major sources for CH_4 in the Indian region are rice, paddies, wetlands and ruminants (Schneising et al., 2009). Annual CH_4 concentration over study area is observed to be 1.92 ± 0.07 ppm, with a maximum (2.02 ± 0.01 ppm) observed in post-monsoon and minimum (1.85 ± 0.03 ppm) in monsoon. The highest concentration appears during post-monsoon and may be associated with the Kharif season (Goroshi et al., 2011). Background (average) values of CH_4 observed during different seasons are 1.93±0.05, 1.89 ± 0.05, 1.85 ± 0.03 and 2.02 ± 7 ppm with respectively winter, pre-monsoon, monsoon and post-monsoon. Low mixing ratios of CH_4 observed during monsoon season were mainly due to the reduction in atmospheric hydrocarbons because of the reduced photochemical reactions and the substantial reduction in solar intensity (Gaur et al., 2014). The rate of change of CH_4 was found to be high during post-monsoon and winter. Both biological and physical processes control the exchange of CH_4 between rice paddy fields and the atmosphere. This may be one of the major reasons for the

ACPD
15, 34205–34241, 2015

enhanced CH_4 observed during post-monsoon and winter seasons (Nishanth et al., 2014).

4.2 Diurnal variations of CO_2 and CH_4

Figure 2c and d depicts seasonal diurnal variations of CO_2 and CH_4 over Shadnagar during study period. The amplitudes diurnal changes during seasonal variation mainly depend on biosphere sources and sinks such as land use land cover change (Fearnside, 2000; IPCC, 1990; Stocker et al., 2013). Maximum mixing ratios of CO_2 and CH_4 are observed during early morning and late night hours. Peak surface concentrations of CO_2 and CH_4 increase at night and remain high until sunrise (22:00 to 06:00 UTC). Figure 2c shows mixing ratios of CO_2 are gradually decreasing after sun rise and reaching peak minimum in the afternoon because of the net ecosystem uptake of the biosphere and boundary layer dynamics. During night time, mixing ratios increase due to formation of stable atmospheric boundary layer, soil respiration of the biosphere and absence of photosynthetic activity. Similar trend in diurnal variation of GHG's is reported from other parts of the country (Patil et al., 2013; Mahesh et al., 2014; Sharma et al., 2014; Nishanth et al., 2014). Although diurnal variations of CH_4 showed similar trend as of CO_2 but are caused due to different factors. Lower troposphere acts as main sink for CH_4 with the formation of O_3 through oxidation of CH_4 and other trace species in the presence of NO_x and hydroxyl radicals ($\dot{O}H$) (Eisele et al., 1997; IPCC, 1990; Stocker et al., 2013).

4.3 Influence of prevailing meteorology

Redistribution (both horizontal and vertical) of GHG's also place a role in their seasonal variation, as it controls transport and diffusion of pollutants from one place to another (Hassan, 2015). A good inverse correlation between wind speed and GHG's suggest the proximity of sources near measurement site, while a not so significant correlation suggest the influence of regional transport (Ramachandran and Rajesh, 2007). Figure 3a and b shows scatter plot between GHG's and wind speed during different seasons. Analysis of Fig. 3 shows that there exist an inverse correlation between monthly mean wind speed and GHG's. Correlation coefficient (R) between wind speed and CO_2 during pre-monsoon, monsoon, post-monsoon and winter is 0.56, 0.32, 0.06 and 0.67 respectively. While for CH_4 it is found be 0.28, 0.71, 0.21, and 0.60 respectively. Negative correlation indicates that the influence of local sources on GHG's, however, poor correlation coefficients during different seasons suggest the role of regional/local transport (Mahesh et al., 2014). Also an understanding of prevailing wind direction and its relationship with GHG's helps in determining their probable source regions. Table 2 shows the monthly mean variation of CO_2 and CH_4 with respect to different wind direction. Enhancement in CO_2 and CH_4 level over Shadnagar are observed to mainly come from NW and NE while the lowest is from the S and SW. This can be associated to some extend with industrial emissions located in western side of sampling site, and the influence of emission and transport from nearby urban center on the NW side of the study site.

The meteorological parameters (temperature and relative humidity) influenceon trace gases is also examined. Figure 4a and b (top panel corresponds to CO_2 and bottom panel represents CH_4) shows the scatter plot of temperature vs. relative humidity as a function of GHGs during different seasons. Here, dailymean data is used instead of hourly mean data, to avoid the influence of the diurnal variations on correlations. CO_2 showed a positive correlation with temperature during all season except during winter. This negative correlation can be attributed to decrease in rate of photosynthesis. IPCC (1990) reports that many mid-latitude plants shows an optimum gross photosynthesis rate when temperature varied from of 20 to 35 °C. The rate of plant respiration tends to be slow below 20 °C. However, at higher temperatures, the respiration rate accelerates rapidly up to a temperature at which, it equals the rate of gross photosynthesis and there can be no net assimilation of carbon. While CH_4 showed a weak positive correlation with temperature during pre-monsoon and post-monsoon, while a weak negative correlation is observed during monsoon and winter. This indicates that regional air tem-

ACPD
15, 34205–34241, 2015

perature does not significantly influence seasonal variation of CH_4 (Chen et al., 2015). Seasonal variation of GHG's also showed an insignificantly negative correlation with relative humidity. A similar observation is also reported by Abhishek et al. (2014). One of the supporting argument can be in humid conditions, these stoma can fully open to increase the uptake of CO_2 without a net water loss. Also, wetter soils can promote decomposition of dead plant materials, releasing natural fertilizers that help plants grow.

Influence of boundary layer height on GHGs mixing ratios

The planetary boundary layer is the lowest layer of the troposphere where wind speed as a function of temperature plays major role in its thickness variation. It is an important parameter for controlling the observed diurnal variations and potentially masking the emissions signal (Newman et al., 2013). Since complete set of COSMIC RO data is not available during the study period, in this analysis we have analysed RO data from July 2013 to June 2014, along with simultaneous observations of GHG's. Monthly variations (Figure not show) of BLH computed from high vertical resolution of COSMIC-RO data against CO_2 and CH_4 concentrations. Monthly BLH is observed to be minimum (maximum) during winter and monsoon (pre monsoon) seasons. The highest (lowest) BLH over study region was identified 3.20 km (1.50 km). An average monthly air temperature is maximum (minimum) of 29 °C (20 °C) during summer (winter) months.

Seasonal change in BLH thickness over study region was observed to be as Monsoon (M, 1.74 km) < winter (W, 2.10 km) < Post Monsoon (PM, 2.30 km) < Pre-monsoon (Pre-M, 3.15 km); its influence on CO_2 and CH_4 mixing ratios are shown in Fig. 5a and b. As seasonal BLH thickness increase, mixing ratios of CO_2 (CH_4) decreased from 8.68 to 5.86 ppm (110 to 40 ppb). The amount of biosphere emissions influence on CO_2 and CH_4 can be estimated through atmospheric boundary layer processes. Since the study region being a flat terrain variations in CO_2 and CH_4 were mostly influenced by boundary layer thickness through convection and biosphere activities.

ACPD
15, 34205–34241, 2015

4.4 Correlation between CO_2 and CH_4

A correlation study is carried out between hourly averaged CO_2 and CH_4 during all season for the entire study period. The statistical analysis for different seasons is shown in Table 3. Fang et al. (2015) suggest that correlation coefficient (R) value higher than 0.50 indicates similar source mechanism of CO_2 and CH_4. Also, a positive correlation dominance of anthropogenic emission on carbon cycle. Our study also reveals a strong positive correlation observed between CO_2 and CH_4 during winter, pre-monsoon, monsoon and post-monsoon with R equal to 0.80, 0.80, 0.61 and 0.72 respectively. Seasonal regression coefficients (slope) and their uncertainties (ψ_{slope}, $\psi_{y\text{-int}}$) are computed using Taylor (1997) which showed maximum during winter, pre-monsoon and minimum in monsoon that figure out the hourly stability of the mixing ratios between CO_2 and CH_4. This can be due to relatively simple source/sink process of CO_2 in comparison with CH_4. Dilution effects during transport of CH_4 and CO_2 can be minimized to some extent by dividing the increase of CH_4 over time by the respective increase in CO_2 (Worthy et al., 2009). Figure 6 shows the seasonal variation of $\Delta CH_4/\Delta CO_2$. In this study, background concentration of respective GHG's are determined as mean values of the 1.25 percentile of data for monsoon, post-monsoon, pre-monsoon and winter (Pan et al., 2011; Worthy et al., 2009). Annual $\Delta CH_4/\Delta CO_2$ over the study region during the study period is found to be 7.1 (ppb ppm^{-1}). This low value clearly indicates the dominance of CO_2 over the study region. The reported $\Delta CH_4/\Delta CO_2$ values from some of the rural sites viz Canadian Arctic and Hateruma Island (China) is of the order 12.2 and $\sim$ 10 ppb ppm^{-1} respectively (Worthy et al., 2009; Tohjima et al., 2014). Average $\Delta CH_4/\Delta CO_2$ ratio during winter, pre-monsoon, monsoon and post-monsoon are 9.40, 6.40, 4.40, and 8.20 ppb respectively. Monthly average, of $\Delta CH_4/\Delta CO_2$, is relatively high from late post-monsoon to winter, when the biotic activity is relatively dormant (Tohjima et al., 2014). During pre-monsoon decease in $\Delta CH_4/\Delta CO_2$ ratio indicates the enhancement of CO_2 relative to that of CH_4.

ACPD
15, 34205–34241, 2015

4.5 Methane (CH_4) sink mechanism

Methane (CH_4) is the most powerful greenhouse gas after CO_2 in the atmosphere due to its strong positive radiative forcing (IPCC, 1990; Stocker et al., 2013). Atmospheric CH_4 is mainly (70–80 %) from biological origin produced in anoxic environments, by anaerobic digestion of organic matter (Crutzen and Zimmermann, 1991). The major CH_4 sink is oxidation by hydroxyl radicals (OH), which accounts for 90 % of CH_4 sink (Vaghjiani and Ravishankara, 1991; Kim et al., 2015). OH radicals are very reactive and are responsible for the oxidation of almost all gases in the atmosphere. Primary source for OH radical formation in the atmosphere is photolysis of ozone (O_3) and water vapor (H_2O). Eisele et al. (1997) defined primary and secondary source of OH radicals in the atmosphere. Primary source of OH radical is as follows;

$$O_3 + h\nu(\lambda \leq 310\,\text{nm}) \rightarrow O_2 + O(^1D) \text{ where } O(^1D) \text{ is electronically excited atom.} \quad (R1)$$

$$O(^1D) + O_2 \rightarrow O + M \quad (R2)$$

$$O(^1D) + H_2O \rightarrow 2OH \text{ primary OH formation.} \quad (R3)$$

Removal of CH_4 is constrained by the presence of OH radicals in the atmosphere. A 1 min time series analysis of CH_4, NO_x, O_3 and H_2O and associated wind vector for August 2014 to understand the CH_4 chemistry is shown in Fig. 7a and b. Low NO_x (1–2 ppb) values are shown in horizontal elliptical region of Fig. 7a and observed corresponding low CH_4 (1.80 ppm) concentrations. The low NO_x in turn produces high OH radicals in the atmosphere due to conversion of HO_2 radical by NO, which removes CH_4 through oxidation process as shown below.

$$HO_2 + NO \rightarrow \dot{O}H + NO_2 \text{ when } NO_x \text{levels 1–2 ppb} \quad (R4)$$

$$CH_4 + \dot{O}H \rightarrow \dot{C}H_3 + H_2O \text{ main } CH_4 \text{ removal process} \quad (R5)$$

$$NO_2 + OH + M \rightarrow HNO_3 + M \text{ if } NO_x > 2 \text{ ppb } (OH\downarrow, CH_4\uparrow) \quad (R6)$$

Crutzen and Zimmermann (1991) and Eisele et al. (1997) observed that at low NO_x (0.5–2.0 ppb) levels most HO_x family radicals such as HO_2 and peroxy radicals (RO_2)

ACPD
15, 34205–34241, 2015

react with NO to form OH radicals. Therefore OH radicals are much higher in the case of low NO_x. When NO_x levels increase more than 2 ppb, most of the OH radicals react with NO_2 to form nitric acid (HNO_3). In first order, the levels of CH_4 in the atmosphere depend on the levels of NO_x though the production of OH radicals in the atmosphere is still uncertain. Figure 7a and b showed high CH_4, H_2O, O_3 and NO_x during a few days in August 2014. High concentrations of CH_4, NO_x and other gases are observed in the eastern direction of study site. Very high NO_x levels above 10 ppb are observed and subsequently CH_4 concentrations also increased to 2.40 from 1.80 ppm. In the eastern direction of study site a national highway and single line broad gauge railway network are present which act as possible sources of NO_x, CH_4 and CO_2. Increase in emissions of NO_x causes decline in the levels of OH radicals and subsequently observed high CH_4 over the study region.

4.6 Influence of vegetation on GHG's.

In India cropping season is classified into (i) Kharif and (ii) Rabi based on the onset of monsoon. The kharif season is from July to October during the south-west monsoon and Rabi season is from October to March (Koshal, 2013). NDVI being one of the indicators of vegetation change, monthly variations of CO_2 and CH_4 against NDVI is studied to understand the impact of land use land cover on mixing ratios of CO_2 and CH_4. Monthly changes in NDVI, CO_2 and CH_4 are shown in Fig. 8. Monthly mean of GHG's represented in this analysis is calculated from daily day time (10:00–16:00 LT) mean. Maximum NDVI of 0.60 corresponding to the minimum CO_2 concentration (about 382 ppm) is observed in September. NDVI showed inverse relationship with CO_2, mainly due to change in vegetation which affects the CO_2 concentrations. CH_4 and NDVI values follow similar trends with highest CH_4 concentrations in October 2014 (about 2.05 ppm) and minimum about 1.80 ppm in July 2014. The main source for CH_4 emissions are soil microbial (Kirschke et al., 2013) activity which are more active during monsoon and post monsoon seasons. High (low) soil moisture and NDVI is observed in monsoon (pre-monsoon) seasons (Figure not show). The predominating factors which

ACPD
15, 34205–34241, 2015

controls the soil emissions of CO_2, CH_4 are moisture content, soil temperature, vegetation and soil respiration (Smith et al., 2003; Jones et al., 2005; Chen et al., 2010) respectively.

Biomass burning (forest fire and crop residue burning) is one of the major sources of gaseous pollutants such as carbon monoxide (CO), methane (CH_4), nitrous oxides (NO_x) and hydrocarbons in the troposphere (Crutzen et al., 1990, 1985; Sharma et al., 2010). In order to study the role of biomass burning on GHG's over study site we have analysed GHG's emissions from biomass burning using long term (2003–2013) Fire Energetics and Emissions Research version 1.0 (FEER v1) data. Emission coefficient (C_e) products during biomass burring is developed from coincident measurements of fire radiative power (FRP) and AOD from MODIS Aqua and Terra satellites (Ichoku and Ellison, 2014). Figure 10 shows seasonal variation of CO_2 emission due to biomass burning over the study site. Enhancement in CO_2 emission is seen during pre-monsoon months; which also supports earlier observation (Fig. 2a). This analysis reveals that biomass burning has a role in pre-monsoon enhancement of CO_2 over study site. For a qualitative analysis of this long range transport, we have analysed air mass trajectories ending over study site during different seasons.

4.7 Long range circulations

To understand the role of long range circulation we separated the trajectory into 4 clusters based on their pathway, namely North-East (N-E), North-West (N-W), South-East (S-E), South-West (S-W). The main criterion of trajectory clustering is to minimize the variability among trajectories and maximize variability among clusters. Cluster mean trajectories of air mass and their percentage contribution to the total calculated for each season over the study period at 3 km altitude are depicted in Fig. 9. Majority of air mass trajectories during winter (~ 44 %), pre-monsoon (~ 64 %), monsoon (~ 80 %) and post-monsoon (~ 41 %) are originating from NW parts of the study site. For a comprehensive analysis, percentage occurrences of cluster mean trajectories of air mass over study area during different season at different altitudes are also tabulated in Ta-

ACPD
15, 34205–34241, 2015

ble 4. During post-monsoon to early pre-monsoon periods which are generally the post-harvest period for some of the crops agriculture residue burning which are quite common in the NW and NE regions part of India (Sharma et al., 2010).Our analysis reveals that during this period majority of air mass reaching the study site at different altitudes come from this part of the country.

5 Conclusions

The present study analysed the seasonal variations of atmospheric GHG's (CO_2 and CH_4) and associated prevailing meteorology over Shadnagar, a suburban site of Central India during the period 2014. The salient findings of the study are the following:

- The annual mean of CO_2 and CH_4 over the study region is found to be 394 ± 2.92 and 1.92 ± 0.07 ppm ($\mu \pm 1\sigma$) respectively. CO_2 and CH_4 showed a significant seasonal variation during the study period. Maximum (Minimum) CO_2 is observed during Pre-monsoon (Monsoon), while CH_4 recorded maximum during post-monsoon and minimum in monsoon. Seasonal analysis of FEER data also showed maximum emission of CO_2 due to biomass burning during pre-monsoon months which indicates the influence of biomass burning on local emissions.
- CO_2 and CH_4 showed consistent diurnal behavior in spite of their significant seasonal variations, with an observed morning (06:00 IST) maxima, followed by afternoon minima (14:00 IST) and enhancing in the late evening ($\sim$ 22:00 IST).
- Correlation coefficient (R) between wind speed and CO_2 during pre-monsoon, monsoon, post-monsoon and winter is 0.56, 0.32, 0.06 and 0.67 respectively. While for CH_4 it is found be 0.28, 0.71, 0.21, and 0.60 respectively. Negative correlation indicates that the influence of local sources on GHG's, however, poor correlation coefficients during different seasons suggest the role of regional/local transport.

ACPD
15, 34205–34241, 2015

- CO_2 showed a positive correlation with temperature during all seasons except during winter. Whereas CH_4 showed a weak positive correlation with temperature during pre-monsoon and post-monsoon, while showing a weak negative correlation during monsoon and winter.
- CO_2 and CH_4 showed a strong positive correlation during winter, pre-monsoon, monsoon and post-monsoon with R equal to 0.80, 0.80, 0.61 and 0.72 respectively. This clearly indicates the seasonal variations in source-sink mechanisms of CO_2 and CH_4 respectively.
- Presence of OH radicals has been implicitly confirmed as a major sink of CH_4 over the study region.

Acknowledgement. This work was part of the Atmospheric CO_2 Retrieval and Monitoring (ACRM) under National Carbon Project (NCP) of ISRO-GBP. We thank D & PQE division of NRSC and P. Sujatha, ACSG for sharing AWS and boundary layer data. The authors sincerely thank the AT-CTM project of ISRO-GBP for providing the O_3 and NO_x analyzers. We would also like to thank MODIS and COSMIC team for providing scientific data sets used in this study.

References

Ao, C. O., Waliser, D. E., Chan, S. K., Li, J. L., Tian, B., Xie, F., and Mannucci, A. J.: Planetary boundary layer heights from GPS radio occultation refractivity and humidity profiles, J. Geophys. Res.-Atmos., 117, D16117, doi:10.1029/2012JD017598, 2012.

Baer, D. S., Paul, J. B., Gupta, M., and O'Keefe, A.: Sensitive absorption measurements in the near-infrared region using off-axis integrated cavity output spectroscopy, in: International Symposium on Optical Science and Technology, International Society for Optics and Photonics, 167–176, 2002.

Berman, E. S., Fladeland, M., Liem, J., Kolyer, R., and Gupta, M.: Greenhouse gas analyzer for measurements of carbon dioxide, methane, and water vapor aboard an unmanned aerial vehicle, Sensor. Actuat. B-Chem., 169, 128–135, 2012.

ACPD

15, 34205–34241, 2015

Chen, H., Wu, N., Wang, Y., and Peng, C.: Methane is an Important Greenhouse Gas. Methane Emissions from Unique Wetlands in China: Case Studies, Meta Analyses and Modelling, Ch. 1, Higher Education Press and Walter de Gruyter GmbH, Berlin/Boston, ISBN 978-3-11-030021-5, 2015.

Crutzen, P. J. and Andreae, M. O.: Biomass burning in the tropics: impact on atmospheric chemistry and biogeochemical cycles, Science, 250, 1669–1678, 1990.

Crutzen, P. J., Delany, A. C., Greenberg, J., Haagenson, P., Heidt, L., Lueb, R., Pollock, W., Seiler, W., Wartburg, A., and Zimmerman, P.: Tropospheric chemical composition measurements in Brazil during the dry season, J. Atmos. Chem., 2, 233–256, 1985.

Draxler, R. R. and Rolph, G. D.: HySPLIT (Hybrid Single Particle Lagrangian Integrated Trajectory) Model access via NOAA ARL READY website, available at: http://www.arl.noaa.gov/ready/hysplit4.html (last access: 31 December 2014), NOAA Air Resources Laboratory, Silver Spring, MD, 2003.

Eisele, F. L., Mount, G. H., Tanner, D., Jefferson, A., Shetter, R., Harder, J. W., and Williams, E. J.: Understanding the production and interconversion of the hydroxyl radical during the Tropospheric OH Photochemistry Experiment, J. Geophys. Res.-Atmos., 102, 6457–6465, 1997.

Fang, S. X., Zhou, L. X., Tans, P. P., Ciais, P., Steinbacher, M., Xu, L., and Luan, T.: In situ measurement of atmospheric CO_2 at the four WMO/GAW stations in China, Atmos. Chem. Phys., 14, 2541–2554, doi:10.5194/acp-14-2541-2014, 2014.

Fang, S. X., Tans, P. P., Steinbacher, M., Zhou, L. X., and Luan, T.: Study of the regional CO_2 mole fractions filtering approach at a WMO/GAW regional station in China, Atmos. Meas. Tech. Discuss., 8, 7057–7091, doi:10.5194/amtd-8-7057-2015, 2015.

Fearnside, P. M.: Global warming and tropical land-use change: greenhouse gas emissions from biomass burning, decomposition and soils in forest conversion, shifting cultivation and secondary vegetation, Climatic Change, 46, 115–158, 2000.

Frankenberg, C., Bergamaschi, P., Butz, A., Houweling, S., Meirink, J. F., Notholt, J., Petersen, A. K., Schrijver, H., Warneke, T., and Aben, I.: Tropical methane emissions: a revised view from SCIAMACHY onboard ENVISA T, Geophys. Res. Lett., 35, L15811, doi:10.1029/2008GL034300, 2008.

Garg, A., Bhattacharya, S., Shukla, P. R., and Dadhwal, V. K.: Regional and sectoral assessment of greenhouse gas emissions in India, Atmos. Environ., 35, 2679–2695, 2001.

ACPD
15, 34205–34241, 2015

Gaur, A., Tripathi, S. N., Kanawade, V. P., Tare, V., and Shukla, S. P.: Four-year measurements of trace gases (SO_2, NO_x, CO, and O_3) at an urban location, Kanpur, in Northern India, J. Atmos. Chem., 71, 283–301, 2014.
Gilmanov, T. G., Johnson, D. A., Saliendra, N. Z., Akshalov, K., and Wylie, B. K.: Gross primary productivity of the true steppe in Central Asia in relation to NDVI: scaling up CO_2 fluxes, Environ. Manage., 33, 492–508, 2004.
Goroshi, S. K., Singh, R. P., Panigrahy, S., and Parihar, J. S.: Analysis of seasonal variability of vegetation and methane concentration over India using SPOT-VEGETATION and ENVISAT-SCIAMACHY data, Journal of the Indian Society of Remote Sensing, 39, 315–321, 2011.
Hassan, A. G. A.: Diurnal and monthly variations in atmospheric CO_2 level in Qena, Upper Egypt, Resources and Environment, 5, 59–65, 2015.
Ichoku, C. and Ellison, L.: Global top-down smoke-aerosol emissions estimation using satellite fire radiative power measurements, Atmos. Chem. Phys., 14, 6643–6667, doi:10.5194/acp-14-6643-2014, 2014.
IPCC: Climate Change: The IPCC Scientific Assessment, edited by: Houghton, J. T., Jerkins, G. J., and Ephraums, J. J., Cambridge University Press, New York, 1990.
James, M. E. and Kalluri, S. N.: The Pathfinder AVHRR land data set: an improved coarse resolution data set for terrestrial monitoring, Int. J. Remote Sens., 15, 3347–3363, 1994.
Jones, C., McConnell, C., Coleman, K., Cox, P., Falloon, P., Jenkinson, D., and Powlson, D.: Global climate change and soil carbon stocks; predictions from two contrasting models for the turnover of organic carbon in soil, Glob. Change Biol., 11, 154–166, 2005.
Keppler, F., Hamilton, J. T., Braß, M. and Röckmann, T.: Methane emissions from terrestrial plants under aerobic conditions, Nature, 439, 187–191, 2006.
Kim, H. S., Chung, Y. S., Tans, P. P., and Dlugokencky, E. J.: Decadal trends of atmospheric methane in East Asia from 1991 to 2013, Air Quality, Atmosphere and Health, 8, 293–298, 2015.
King, M. D., Kaufman, Y. J., Menzel, W. P., and Tanre, D.: Remote sensing of cloud, aerosol, and water vapor properties from the Moderate Resolution Imaging Spectrometer (MODIS), IEEE T. Geosci. Remote , 30, 2–27, 1992.
Kirschke, S., Bousquet, P., Ciais, P., Saunois, M., Canadell, J. G., Dlugokencky, E. J., Bergamaschi, P., Bergmann, D., Blake, D. R., Bruhwiler, L., Cameron-Smith, P., Castaldi, S., Chevallier, F., Feng, L., Fraser, A., Heimann, M., Hodson, E. L., Houweling, S., Josse, B., Fraser, P. J., Krummel, P. B., Lamarque, J.-F., Langenfelds, R. L., Quéré, C. L., Naik, V., O'Doherty,

ACPD
15, 34205–34241, 2015

S., Palmer, P. I., Pison, I., Plummer, D., Poulter, B., Prinn, R. G., Rigby, M., Ringeval, B., Santini, M., Schmidt, M., Shindell, D. T., Simpson, I. J., Spahni, R., Steele, L. P., Strode, S. A., Sudo, K., Szopa, S., van der Werf, G. R., Voulgarakis, A., Weele, M., Weiss, R. F., Williams, J. E., and Guang, Z.: Three decades of global methane sources and sinks, Nat. Geosci., 6, 813–823, doi:10.1038/NGEO1955, 2013.

Koshal, A. K.: Spatial temporal climatic change variability of cropping system in western Uttar Pradesh, Int. J. Remote Sens. Geosci., 2, 36–45, 2013.

Lewis, A. C., Evans, M. J., Hopkins, J. R., Punjabi, S., Read, K. A., Purvis, R. M., Andrews, S. J., Moller, S. J., Carpenter, L. J., Lee, J. D., Rickard, A. R., Palmer, P. I., and and Parrington, M.: The influence of biomass burning on the global distribution of selected non-methane organic compounds, Atmos. Chem. Phys., 13, 851–867, doi:10.5194/acp-13-851-2013, 2013.

Machida, T., Kita, K., Kondo, Y., Blake, D., Kawakami, S., Inoue, G., and T. Ogawa.: Vertical and meridional distributions of the atmospheric CO_2 mixing ratio between northern midlatitudes and southern subtropics, J. Geophys. Res.-Atmos., 107, 1984–2012, 2002.

Mahesh, P., Sharma, N., Dadhwal, V. K., Rao, P. V. N., and Apparao, B. V.: Impact of land–sea breeze and rainfall on CO_2 variations at a coastal station, J. Earth Sci. Clim. Change, 5, 201, doi:10.4172/2157-7617.1000201, 2014.

Mahesh, P., Sreenivas, G., Rao, P. V. N., Dadhwal, V. K., Sai Krishna, S. V. S., and Mallikarjun, K.: High precision surface level CO_2 and CH_4 using Off-Axis Integrated Cavity Output Spectroscopy (OA-ICOS) over Shadnagar, India, Int. J. Remote Sens., 36, 5754–5765, doi:10.1080/01431161.2015.1104744, 2015.

Miller, J. B., Gatti, L. V., d'Amelio, M. T. S., Crotwell, A. M., Dlugokencky, E. J., Bakwin, P., Artaxo, P., and Tans, P. P.: Airborne measurements indicate large methane emissions from the eastern Amazon basin, Geophys. Res. Lett., 34, L10809, doi:10.1029/2006GL029213, 2007.

Monastersky, R.: Global carbon dioxide levels near worrisome milestone, Nature, 497, 13–14, 2013.

Newman, S., Jeong, S., Fischer, M. L., Xu, X., Haman, C. L., Lefer, B., Alvarez, S., Rappenglueck, B., Kort, E. A., Andrews, A. E., Peischl, J., Gurney, K. R., Miller, C. E., and Yung, Y. L.: Diurnal tracking of anthropogenic CO_2 emissions in the Los Angeles basin megacity during spring 2010, Atmos. Chem. Phys., 13, 4359–4372, doi:10.5194/acp-13-4359-2013, 2013.

ACPD
15, 34205–34241, 2015

Influence of meteorology on GHGs and their interrelationship

G. Sreenivas et al.

Nishanth, T., Praseed, K. M., Satheesh Kumar, M. K., and Valsaraj, K. T.: Observational study of surface O_3, NO_x, CH_4 and total NMHCs at Kannur, India, Aerosol Air Qual. Res., 14, 1074–1088, 2014.

Pan, X. L., Kanaya, Y., Wang, Z. F., Liu, Y., Pochanart, P., Akimoto, H., Sun, Y. L., Dong, H. B., Li, J., Irie, H., and Takigawa, M.: Correlation of black carbon aerosol and carbon monoxide in the high-altitude environment of Mt. Huang in Eastern China, Atmos. Chem. Phys., 11, 9735–9747, doi:10.5194/acp-11-9735-2011, 2011.

Patil, M. N., Dharmaraj, T., Waghmare, R. T., Prabha, T. V., and Kulkarni, J. R.: Measurements of carbon dioxide and heat fluxes during monsoon-2011 season over rural site of India by eddy covariance technique, J. Earth Syst. Sci., 123, 177–185, 2014.

Paul, J. B., Lapson, L., and Anderson, J. G.: Ultrasensitive absorption spectroscopy with a high-finesse optical cavity and off-axis alignment, Appl. Optics, 40, 4904–4910, 2001.

Pielke, R. A., Marland, G., Betts, R. A., Chase, T. N., Eastman, J. L., Niles, J. O., and Running, S. W.: The influence of land-use change and landscape dynamics on the climate system: relevance to climate-change policy beyond the radiative effect of greenhouse gases, Philos. T. Roy. Soc. A, 360, 1705–1719, 2002.

Ramachandran, S. and Rajesh, T. A.: Black carbon aerosol mass concentrations over Ahmedabad, an urban location in western India: comparison with urban sites in Asia, Europe, Canada, and the United States, J. Geophys. Res.-Atmos., 112, D06211, doi:10.1029/2006JD007488, 2007.

Salomonson, V. V., Barnes, W. L., Maymon, P. W., Montgomery, H. E., and Ostrow, H.: MODIS: Advanced facility instrument for studies of the Earth as a system, IEEE T. Geosci. Remote, 27, 145–153, 1989.

Schneising, O., Buchwitz, M., Burrows, J. P., Bovensmann, H., Bergamaschi, P., and Peters, W.: Three years of greenhouse gas column-averaged dry air mole fractions retrieved from satellite – Part 2: Methane, Atmos. Chem. Phys., 9, 443–465, doi:10.5194/acp-9-443-2009, 2009.

Anu Rani Sharma, Shailesh Kumar Kharol, Badarinath, K. V. S., and Darshan Singh: Impact of agriculture crop residue burning on atmospheric aerosol loading –a study over Punjab State, India, Ann. Geophys., 28, 367–379, doi:10.5194/angeo-28-367-2010, 2010.

Sharma, N., Nayak, R. K., Dadhwal, V. K., Kant, Y., and Ali, M. M.: Temporal variations of atmospheric CO_2 in Dehradun, India during 2009, Air, Soil and Water Res., 6, 37–45, doi:10.4137/ASWR.S10590, 2013.

Sharma, N., Dadhwal, V. K., Kant, Y., Mahesh, P., Mallikarjun, K., Gadavi, H., Sharma, A., and Ali, M. M.: Atmospheric CO_2 Variations in Two Contrasting Environmental Sites Over India, Air, Soil and Water Res., 7, 61–68, doi:10.4137/ASWR.S13987, 2014.

Smith, K. A., Ball, T., Conen, F., Dobbie, K. E., Massheder, J., and Rey, A.: Exchange of greenhouse gases between soil and atmosphere: interactions of soil physical factors and biological processes, Eur. J. Soil Sci., 54, 779–791, 2003.

Stocker, T. F., Qin, D., Plattner, G. K., Alexander, L. V., Allen, S. K., Bindoff, N. L., Bréon, F. M., Church, J. A., Cubasch, U., Emori, S., Forster, P., Friedlingstein, P., Gillett, N., Gregory, J. M., Hartmann, D. L., Jansen, E., Kirtman, B., Knutti, R., Krishna Kumar, K., Lemke, P., Marotzke, J., Masson-Delmotte, V., Meehl, G. A., Mokhov, I. I., Piao, S., Ramaswamy, V., Randall, D., Rhein, M., Rojas, M., Sabine, C., Shindell, D., Talley, L. D., Vaughan D. G., and Xie, S. P.: Technical summary, in: Climate Change 2013: The Physical Science Basis, Contribution of Working Group I to the Fifth Assessment Report of the Intergovernmental Panel on Climate Change, edited by: Stocker, T. F., Qin, D., Plattner, G.-K., Tignor, M., Allen, S. K., Boschung, J., Nauels, A., Xia, Y., Bex, V., and Midgley, P. M., Cambridge University Press, Cambridge, UK and New York, NY, USA, 2013.

Stohl, A., Hittenberger, M., and Wotawa, G.: Validation of the Lagrangian particle dispersion model FLEXPART against large-scale tracer experiment data, Atmos. Environ., 32, 4245–4264, 1998.

Taylor, J.: An Introduction to Error Analysis: The Study of Uncertainties in Physical Measurement, University Science Books, Sausalito, CA, 1997.

Thum, T., Aalto, T., Laurila, T., Aurela, M., Hatakka, J., Lindroth, A., and Vesala, T.: Spring initiation and autumn cessation of boreal coniferous forest CO_2 exchange assessed by meteorological and biological variables, Tellus B, 61, 701–717, 2009.

Tohjima, Y., Kubo, M., Minejima, C., Mukai, H., Tanimoto, H., Ganshin, A., Maksyutov, S., Katsumata, K., Machida, T., and Kita, K.: Temporal changes in the emissions of CH_4 and CO from China estimated from CH_4/CO_2 and CO/CO_2 correlations observed at Hateruma Island, Atmos. Chem. Phys., 14, 1663–1677, doi:10.5194/acp-14-1663-2014, 2014.

Vaghjiani, G. L. and Ravishankara, A. R.: New measurement of the rate coefficient for the reaction of OH with methane, Nature, 350, 406–409, 1991.

Wang, B.-R., Liu, X.-Y., and Wang, J.-K.: Assessment of COSMIC radio occultation retrieval product using global radiosonde data, Atmos. Meas. Tech., 6, 1073–1083, doi:10.5194/amt-6-1073-2013, 2013.

Worthy, D. E. J., Chan, E., Ishizawa, M., Chan, D., Poss, C., Dlugokencky, E. J., Maksyutov, S., and Levin, I.: Decreasing anthropogenic methane emissions in Europe and Siberia inferred from continuous carbon dioxide and methane observations at Alert, Canada, J. Geophys. Res.-Atmos., 114, D10301, doi:10.1029/2008JD011239, 2009.

Yang, L., Wang, X., Guo, M., Tani, H., Matsuoka, N., and Matsumura, S.: Spatial and temporal relationships among NDVI, climate factors, and land cover changes in Northeast Asia from 1982 to 2009, GIScience and Remote Sensing, 48, 371–393, doi:10.2747/1548-1603.48.3.371, 2011.

Yunck, T. P., Liu, C.-H., and Ware, R.: A history of GPS sounding, Terr. Atmos. Ocean Sci., 11, 1–20, 2000.

ACPD
15, 34205–34241, 2015

Table 1. Data used.

Sensor	Period	Parameter	resolution	Source
GGA-24EP	Jan 2014 to Dec 2014	CO_2,CH_4 and H_2O	1 Hz time	ASL, NRSC
42i-NO-NO_2-NO_x	Jul 2014 to Sep 2014	NO_x(= NO + NO_2)	1 min time	ASL, NRSC
49i-O_3	Jul 2014 to Sep 2014	O_3	1 min time	ASL, NRSC
AWS	Jan 2014 to Dec 2014	WS, WD, AT, RH	60 min time	NRSC
Terra/MODIS	Jan 2014 to Dec 2014	NDVI	5 km horizontal	http://ladsweb.nascom.nasa.gov/data/search.html
COSMIC-1DVAR	Jul 2013 to Jun 2014	Refractivity (N)	0.1 km vertical	
HYSPLIT	Jan 2014 to Dec 2014	Backward trajectory	5 day isentropic model (1 to 4 km)	http://www.arl.noaa.gov/ready/hysplit4.html
FEER v1	Jan 2003 to Dec 2013	fire radiative power (FRP)		http://ladsweb.nascom.nasa.gov/data/search.html

ACPD
15, 34205–34241, 2015

Table 2. Seasonal amplitudes of CO_2 and CH_4 over study region arriving from different directions.

Wind Direction	Winter $\frac{CO_2}{CH_4}$ (ppm)	Pre-monsoon $\frac{CO_2}{CH_4}$ (ppm)	Monsoon $\frac{CO_2}{CH_4}$ (ppm)	Post-monsoon $\frac{CO_2}{CH_4}$ (ppm)
0–45	399.85/1.98	410.37/1.94	400.72/1.91	395.13/2.02
45–90	391.66/1.94	399.59/1.89	388.82/1.91	390.23/1.98
90–135	391.57/1.93	397.79/1.87	388.99/1.87	389.06/1.97
135–180	389.34/1.89	393.87/1.85	391.81/1.86	387.69/1.97
180–225	391.14/1.89	396.75/1.85	390.28/1.82	392.30/2.02
225–270	389.13/1.88	394.81/1.86	390.26/1.82	384.40/1.94
270–315	388.68/1.87	398.68/1.89	389.58/1.82	384.99/1.93
315–360	390.87/1.91	401.17/1.89	387.58/1.83	389.32/1.98

ACPD
15, 34205–34241, 2015

Table 3. Statistical correlation between CO_2 and CH_4.

S.No	Seasons	Correlation coefficient $\left(R^2\right)$	Slope $\left(\frac{Y_{CH_4}\text{ (ppm)}}{X_{CO_2}\text{ (ppm)}}\right)$	ψ_{slope} (ppm)	$\Psi_{y\text{-int}}$ (ppm)
1	Monsoon (JJAS)	0.37	0.005	0.00015	1.91
2	Post-monsoon (OND)	0.52	0.0065	0.00014	1.52
3	Winter (JF)	0.61	0.0085	0.00018	9.13
4	Pre-monsoon (MAM)	0.64	0.0059	0.00021	2.73

ACPD
15, 34205–34241, 2015

Table 4. Cluster analysis of air mass trajectories reaching Shadnagar at various heights during different seasons.

Seasonal Backward	NW				NE				SE				SW			
trajectory (%)	1 km	2 km	3 km	4 km	1 km	2 km	3 km	4 km	1 km	2 km	3 km	4 km	1 km	2 km	3 km	4 km
Winter	54	32	2	0	32	24	44	52	10	25	11	7	4	19	42	41
Pre-monsoon	24	9	8	1	26	31	64	78	36	46	2	10	14	14	26	11
Monsoon	0	1	7	19	12	34	80	70	4	4	4	6	84	61	9	5
Post-monsoon	42	15	11	14	47	53	41	49	8	30	32	26	3	2	16	11

ACPD
15, 34205–34241, 2015

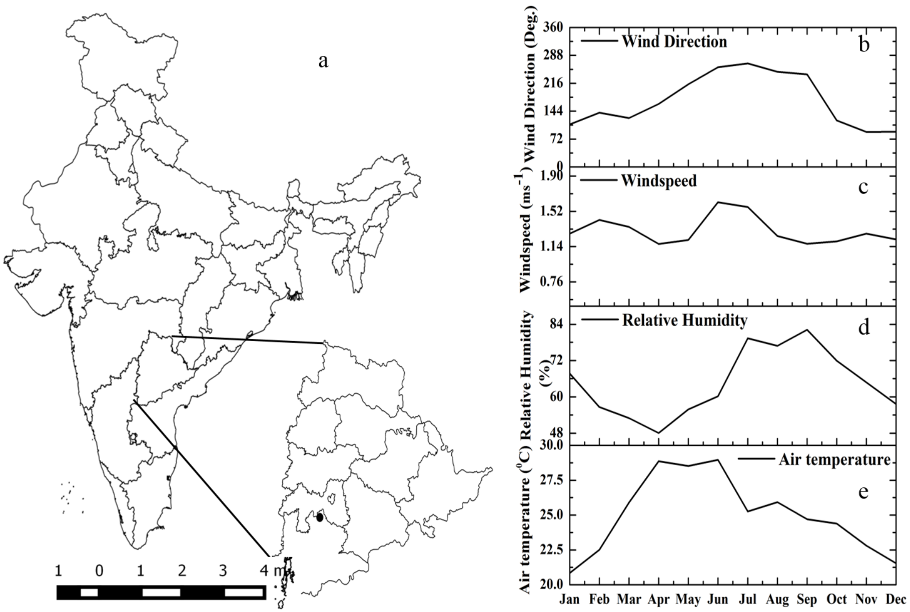

Figure 1. (a) Schematic representation of study area; **(b–e)** Seasonal variation of prevailing meteorological conditions during study period.

ACPD
15, 34205–34241, 2015

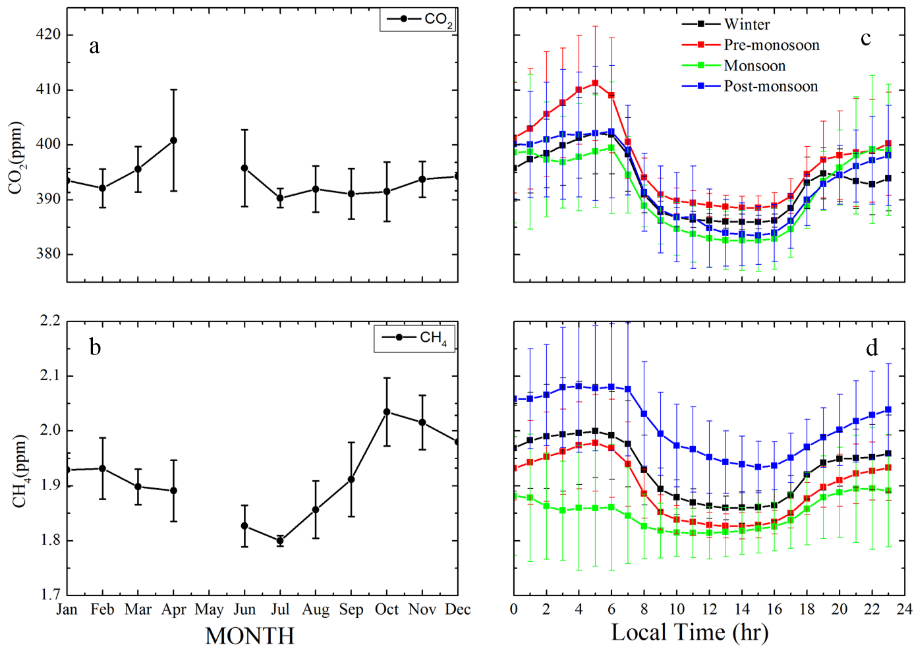

Figure 2. (a–b) Seasonal variations of CO_2 and CH_4; **(c–d)** diurnal variations of CO_2 and CH_4 during 2014.

ACPD
15, 34205–34241, 2015

Influence of meteorology on GHGs and their interrelationship

G. Sreenivas et al.

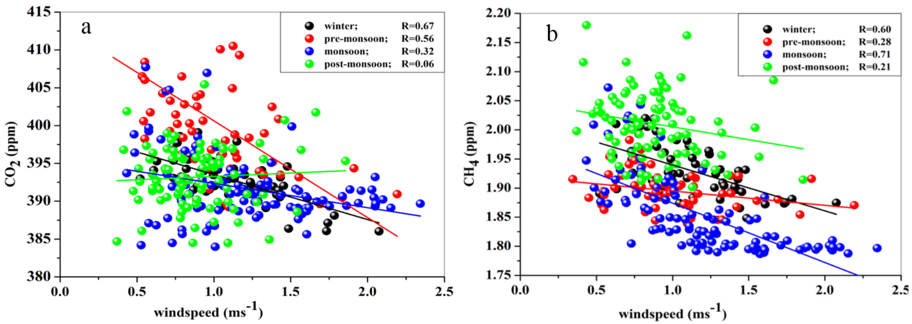

Figure 3. (a–b) Scatterplot between wind speed and GHG's (CO_2 and CH_4).

ACPD
15, 34205–34241, 2015

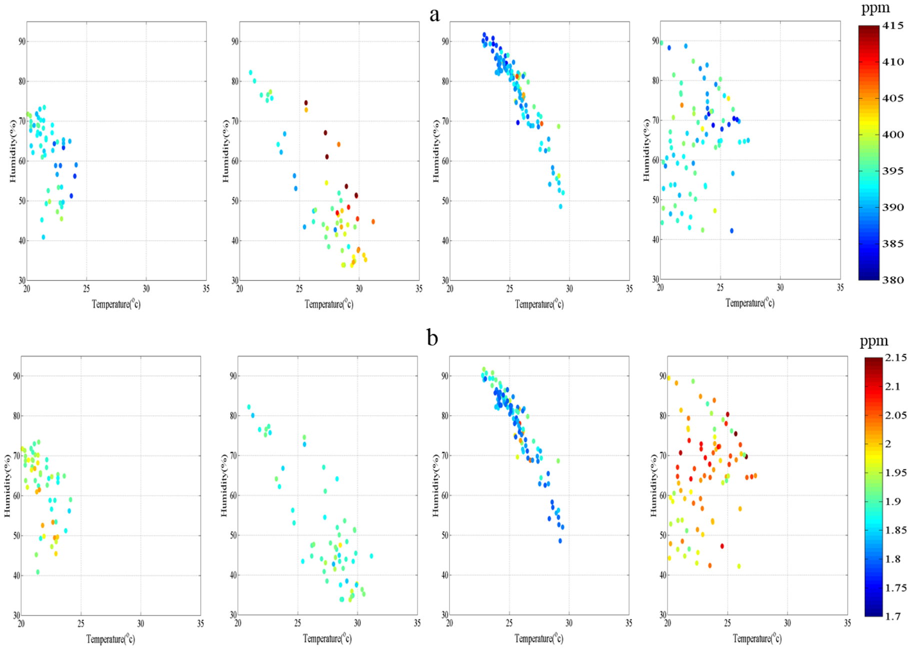

Figure 4. (a) Seasonal variation of CO_2 as function of humidity and temperature during winter, pre-monsoon, monsoon and post-monsoon. **(b)** Seasonal variation of CH_4 as function of humidity and temperature during respective seasons.

ACPD
15, 34205–34241, 2015

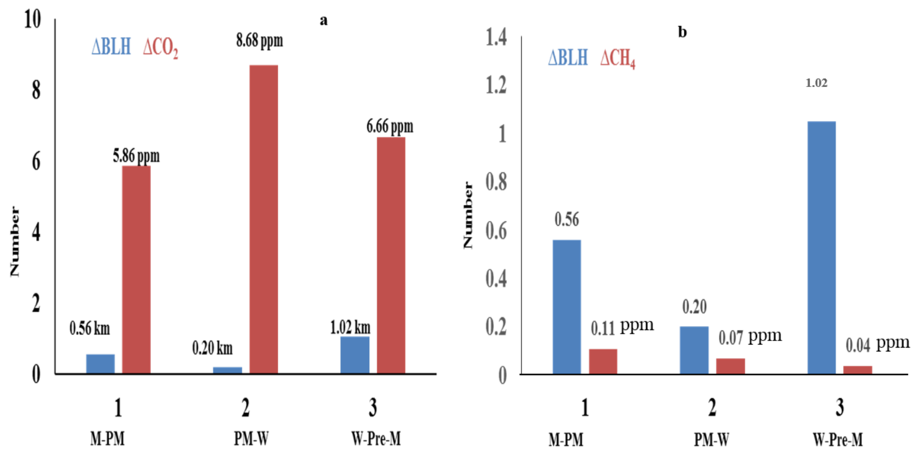

Figure 5. Seasonal variations of **(a)** CO_2 and **(b)** CH_4 against boundary layer height change.

ACPD
15, 34205–34241, 2015

Influence of meteorology on GHGs and their interrelationship

G. Sreenivas et al.

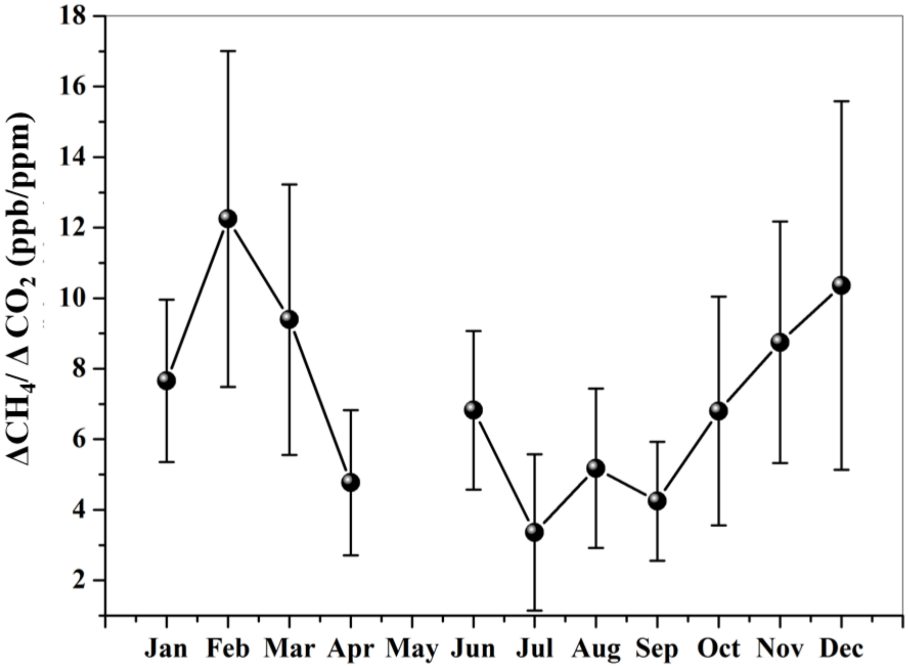

Figure 6. Monthly variation of $\Delta CH_4/\Delta CO_2$ during study period.

ACPD
15, 34205–34241, 2015

Influence of meteorology on GHGs and their interrelationship

G. Sreenivas et al.

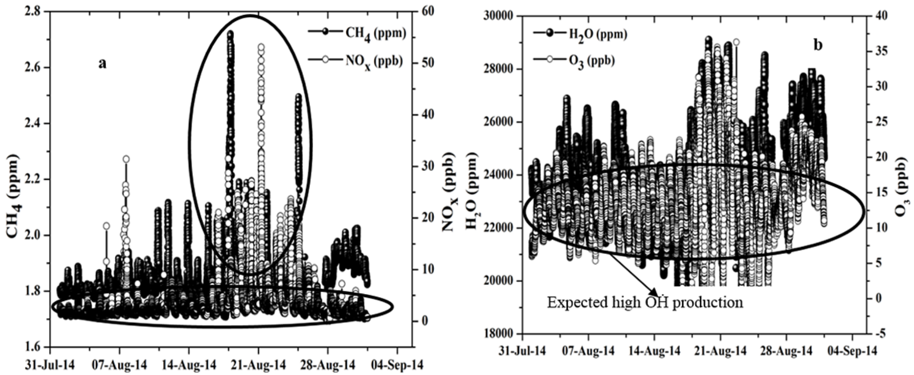

Figure 7. Time series analysis of **(a)** CH_4 vs. NO_x, **(b)** H_2O vs. O_3.

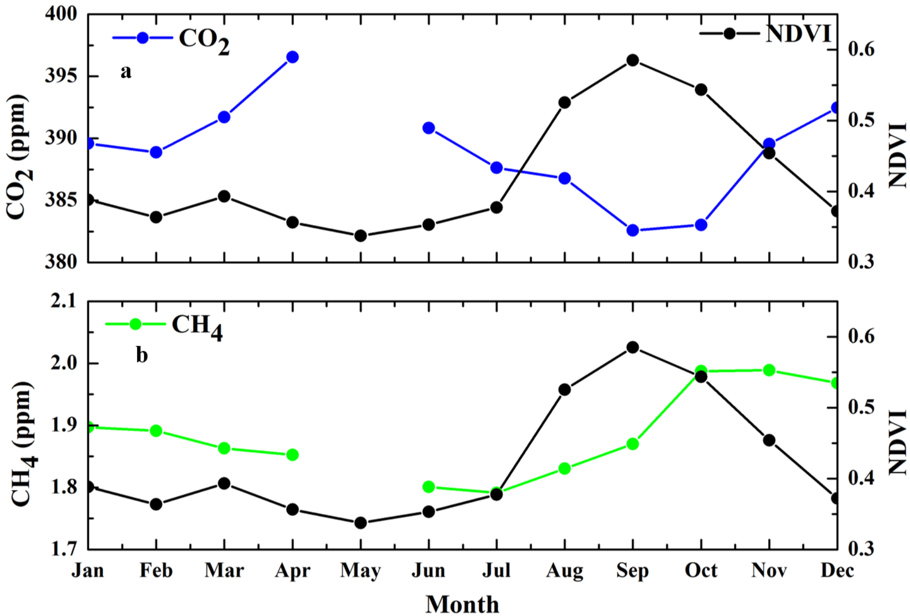

Figure 8. (a) Seasonal variation of CO_2 in conjunction with NDVI (Normalized Difference Vegetation Index). **(b)** Seasonal variation of CH_4 in conjunction with NDVI.

ACPD
15, 34205–34241, 2015

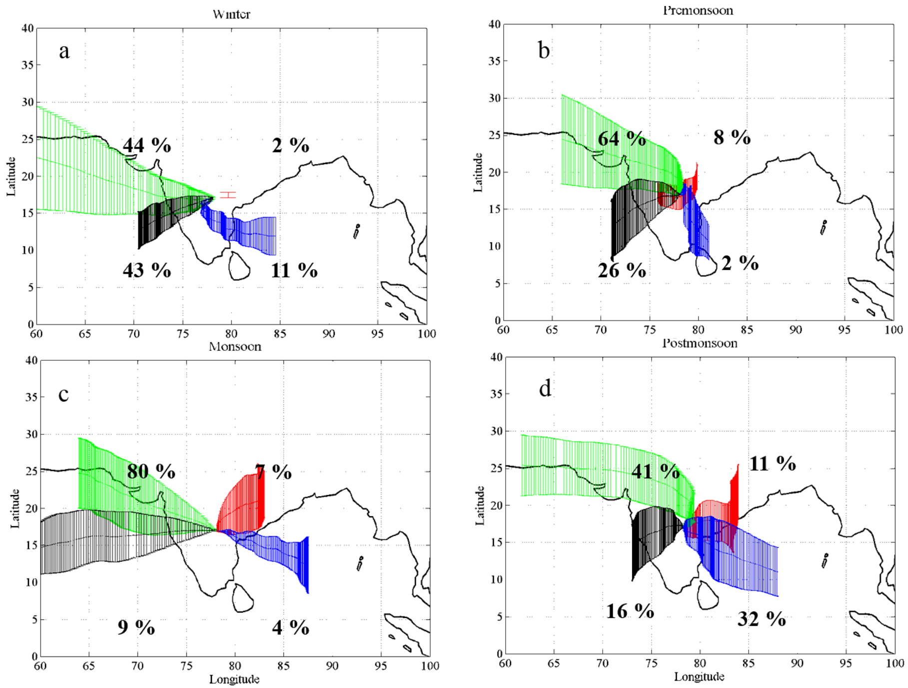

Figure 9. (a–d) Long range circulation of air mass trajectories ending over Shadnagar at 3 km during winter, pre-monsoon, monsoon and post-monsoon.

ACPD
15, 34205–34241, 2015

Influence of meteorology on GHGs and their interrelationship

G. Sreenivas et al.

Title Page
Abstract Introduction
Conclusions References
Tables Figures
◀◀ ▶▶
◀ ▶
Back Close
Full Screen / Esc
Printer-friendly Version
Interactive Discussion

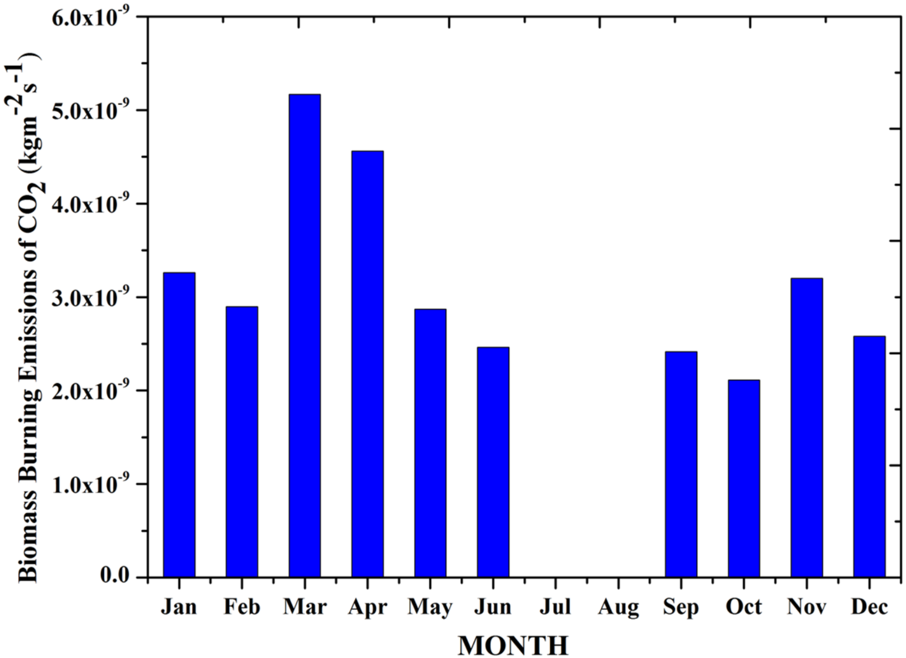

Figure 10. Long term analysis of CO_2 biomass burning emissions over study region.

ACPD
15, 34205–34241, 2015

Influence of meteorology on GHGs and their interrelationship

G. Sreenivas et al.